CZASOPISMO TECHNICZNE Ś
WYDAWNICTWO POLITECHNIKI KRAKOWSKIEJ

z. 3-Ś/2008
ISSN 0011-4561
ISSN 1897-6336

TOMASZ ŻEBRO*, KATARZYNA KOWALCZYK-GAJEWSKA**, JERZY PAMIN*

A GEOMETRICALLY NONLINEAR MODEL OF SCALAR DAMAGE COUPLED TO PLASTICITY

GEOMETRYCZNIE NIELINIOWY MODEL SKALARNEGO USZKODZENIA SPRZĘŻONEGO Z PLASTYCZNOŚCIĄ

Abstract

The paper presents a coupled damage-plasticity model at large strain, based on the multiplicative split of the deformation gradient into elastic and plastic parts and incorporating plasticity-induced isotropic damage. Attention is focused on an efficient implementation in the FEAP finite element package. Numerical simulations of two benchmarks are performed and possibilities of gradient enhancement are considered.

Keywords: damage, plasticity, large strain

Streszczenie

W artykule przedstawiono teorię sprzężonej plastyczności i uszkodzenia przy założeniu dużych odkształceń. Jest ona oparta na iloczynowym rozkładzie gradientu deformacji na część sprężystą i plastyczną. Uwzględnia izotropowe uszkodzenie wywołane wzrostem odkształceń plastycznych. Uwagę skupiono na efektywnej implementacji sformułowania w pakiecie FEAP, opartym na metodzie elementów skończonych. Wykonano symulacje numeryczne dwu przykładowych testów. Rozważono możliwości wprowadzenia do modelu członu gradientowego.

Słowa kluczowe: uszkodzenie, plastyczność, duże odkształcenia

*Mgr Tomasz Żebro, Dr hab. Jerzy Pamin, Institute for Computational Civil Engineering, Faculty of Civil Engineering, Cracow University of Technology, Cracow, Poland.
**Dr Katarzyna Kowalczyk-Gajewska, Institute of Fundamental Technological Research PAS, Warsaw, Poland.

1. Introduction

There is a vast literature on coupled damage-plasticity models with linear kinematics. Such models have important advantages in numerical modelling of composites: void or crack growth, irreversible deformations and stiffness degradation can be properly represented while the theory is relatively simple. If applied to localized failure, the model requires regularization which is commonly performed as a nonlocal enhancement, having either gradient or integral form.

The whole description becomes much more complex when a geometrically nonlinear problem is analyzed. The aim of the article is to present some options of gradient plasticity and damage modelling at large strain, based on the multiplicative split of the deformation gradient into elastic and plastic parts and incorporating plasticity-induced isotropic damage. Attention is focused on efficient implementation in the FEAP finite element package. The possibilities of gradient enhancement are considered. The paper is based on the concepts presented in papers [1, 2]. In particular, the approach of [2] is simplified and applied in numerical simulations of benchmarks of distributed and localized deformation (one-element test, perforated plate under tension).

2. Isotropic large deformation elastic-plastic model

The analysis departs from the model of Auricchio and Taylor [1]. A continuous elastic-plastic body under large deformations is considered. Adopting the standard multiplicative decomposition of the deformation gradient $\mathbf{F}$ into elastic and plastic factors $\mathbf{F}^{\mathrm{e}}$ and $\mathbf{F}^{\mathrm{p}}$, i.e.

$$\mathbf{F} = \mathbf{F}^{\mathrm{e}}\mathbf{F}^{\mathrm{p}} \tag{1}$$

we employ the elastic left Cauchy-Green tensor $\mathbf{b}^{\mathrm{e}}$ and the plastic right Cauchy-Green tensor $\mathbf{C}^{\mathrm{p}}$

$$\mathbf{b}^{\mathrm{e}} = \mathbf{F}^{\mathrm{e}}\mathbf{F}^{\mathrm{eT}}, \quad \mathbf{C}^{\mathrm{p}} = \mathbf{F}^{\mathrm{pT}}\mathbf{F}^{\mathrm{p}} \tag{2}$$

By computing $\mathbf{F}^{\mathrm{e}}$ from eq. (1) and substituting into eq. $(2)_1$ it can be shown that the two tensors are related by

$$\mathbf{b}^{\mathrm{e}} = \mathbf{F}[\mathbf{C}^{\mathrm{p}}]^{-1}\mathbf{F}^{\mathrm{T}} \tag{3}$$

and hence tensor $\mathbf{b}^{\mathrm{e}}$ plays the role of internal variable.

The interest is limited to isotropic response and the Kirchhoff stress is defined as

$$\tau = 2\frac{\partial \psi}{\partial \mathbf{b}^{\mathrm{e}}}\mathbf{b}^{\mathrm{e}} \tag{4}$$

where ψ is the Helmholtz free energy, which for the simple case of elastic-plastic material with isotropic hardening parametrized by κ, reads

$$\psi = \psi(\mathbf{b}^{\mathrm{e}}, \kappa) \tag{5}$$

Its convenient form is adopted from [1] and, limiting consideration to linear hardening, augmented by a quadratic function of parameter κ.

Since the principal directions of tensors $\mathbf{b}^{\mathrm{e}}$ and τ coincide, their spectral decomposition is performed using the same vectors $\mathbf{n}^A$. Denoting the elastic stretches by λ^{e}_A we can write that

$$\tau = \sum_{A=1}^{3} \tau_A \mathbf{n}_A \otimes \mathbf{n}_A \tag{6}$$

and

$$\tau_A = \frac{\partial \psi}{\partial \lambda^{\mathrm{e}}_A} \lambda^{\mathrm{e}}_A \tag{7}$$

We consider the simplest case of Huber-Hencky-Mises (HMH) plasticity, so that the yield function ϕ is written in the space of Kirchhoff stresses

$$\phi(\tau, \kappa) = \sqrt{2J_2^{\tau}} - \sqrt{2/3} q(\kappa) \tag{8}$$

However, the reasoning holds for more complex yield functions, cf. [1].

We write the evolution of $\mathbf{b}^{\mathrm{e}}$ in terms of its Lie derivative:

$$\pounds_{\mathbf{v}} \mathbf{b}^{\mathrm{e}} = \mathbf{F}^T \frac{\partial}{\partial t} \left[(\mathbf{C}^p)^{-1} \right] \mathbf{F} \tag{9}$$

The associated flow rule thus reads:

$$-\frac{1}{2} \pounds_{\mathbf{v}} \mathbf{b}^{\mathrm{e}} = \dot{\gamma} \mathbf{N} \mathbf{b}^{\mathrm{e}} \tag{10}$$

where $\dot{\gamma}$ is a plastic multiplier, tensor $\mathbf{N} = \frac{\partial \phi}{\partial \tau}$ denotes the direction of plastic flow, (in the case of HMH plasticity the direction tensor is defined as $\mathbf{N} = \frac{\partial F}{\partial J_2^{\tau}} \tau'$, where τ' is the deviatoric part of the Kirchhoff tensor). The Kuhn-Tucker conditions hold

$$\dot{\gamma} \geq 0, \;\; \phi \leq 0, \;\; \dot{\gamma} \phi = 0 \tag{11}$$

In the simplest case the hardening parameter $\dot{\kappa}$ is identified with the plastic multiplier.

To integrate the nonlinear problem in time, we follow the approach pioneered by Simo [3] in order to preserve the convenient small-strain structure of return mapping algorithm, see also [1]. We denote by t_n (and subscript n) the time moment when the solution is known: thus $\mathbf{F}_n$ and $\mathbf{b}^{\mathrm{e}}_n$ are given. Further, we denote by $t = t_{n+1}$ (subscript $n+1$ or, for simplicity, no subscript) the current time moment ($t - t_n = \Delta t > 0$), for which in the deformation-driven approach $\mathbf{F} = \mathbf{F}_{n+1}$ is also known.

The relative deformation gradient is introduced (see Fig. 1)

$$\mathbf{F} = \mathbf{f} \mathbf{F}_n \tag{12}$$

and the classical elastic predictor – plastic corrector approach is followed. First the trial update of the elastic Cauchy-Green tensor is computed at time t_n assuming that the plastic deformation does not grow in the current time step, i.e. is assumed to be elastic

$$\mathbf{b}^{\mathrm{e}}_{tr} = \mathbf{f} \mathbf{b}^{\mathrm{e}}_n \mathbf{f}^T \tag{13}$$

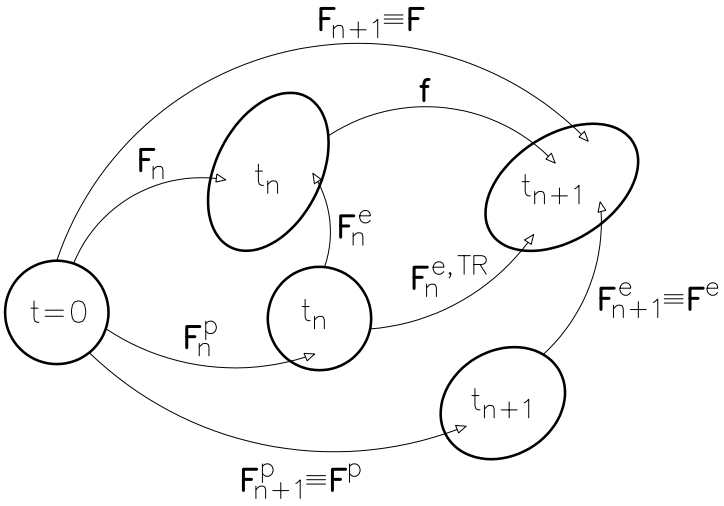

Fig. 1. Decomposition of deformation gradient at time moments n and $n+1$
Rys. 1. Rozkład gradientu deformacji w chwilach czasu n i $n+1$

Then, if the yield condition is violated, the evolutionary problem of plasticity is solved basing on the trial solution

$$\dot{\mathbf{b}}^{\mathrm{e}} = -2\dot{\gamma}\mathbf{N}\mathbf{b}^{\mathrm{e}}_{tr} \tag{14}$$

Time integration of eq. (14) using exponential approximation gives the update of $\mathbf{b}^{\mathrm{e}}$ (see also [3, 1])

$$\mathbf{b}^{\mathrm{e}} = \exp(-2\Delta\gamma\mathbf{N})\mathbf{b}^{\mathrm{e}}_{tr} \tag{15}$$

Since the material is assumed to be isotropic and tensors $\mathbf{b}^{\mathrm{e}}$, $\mathbf{b}^{\mathrm{e}}_{tr}$ and $\mathbf{N}$ have the same eigenvectors $\mathbf{n}_A$ and the computations can be performed in the space of principal directions using vectors with three components. Using logarithmic stretches (Hencky strains) defined as

$$\varepsilon^e_A = \log(\lambda^e_A) \tag{16}$$

we can write

$$\varepsilon^{\mathrm{e}}_A = \varepsilon^{\mathrm{e}}_{A,tr} - \Delta\gamma\mathbf{N}_A \tag{17}$$

which resembles the small-strain return mapping format written in terms of elastic strains.

It is stressed that the algorithm requires the solution of a nonlinear system of four equations, i.e. eq. (17) and (8) at every integration point, which is performed as shown in [1]. The Cauchy stress and material tangent is then computed. At the global level of Newton-Raphson iterations consistent linearization is recommended, cf. [4, 5].

3. Simple coupling with damage

We now couple the model presented in the previous section with the concept of isotropic damage limited to one scalar parameter D which is zero for intact material and grows to one as microcracks and microvoids form progressively during deformation. The damage growth process is assumed to be driven by plastic strains and starts when the hardening parameter κ, identified for simplicity with the plastic multiplier γ, exceeds the assumed value of damage threshold κ_D. We thus postulate the Helmholtz free energy in the form

$$\psi = (1-D)\psi^{\mathrm{e}}(\mathbf{b}^{\mathrm{e}}) + \psi^{\mathrm{p}}(\kappa) \tag{18}$$

We introduce the concept of effective Kirchhoff stress $\hat{\tau}$

$$\tau = (1-D)\hat{\tau} \tag{19}$$

and thermodynamic force Y conjugate to damage, which is the strain energy release measure:

$$Y = -\frac{\partial \psi}{\partial D} = \psi^{\mathrm{e}} \tag{20}$$

Three options of damage growth law are considered. According to the thermodynamically motivated model of Lemaitre [7] the rate of damage is computed as

$$\dot{D} = \frac{\dot{\kappa}}{(1-D)}\frac{Y}{Y_0}$$

where Y_0 is a material parameter (energy strength of damage). The damage growth is determined by strain energy Y and equivalent plastic strain κ. In [6] the damage growth with a different kinetics was assumed

$$\dot{D} = \dot{\kappa}(1-D)\frac{Y}{Y_0} \tag{21}$$

This option is called modified damage-plasticity in further tests. The third option is the following exponential model [8]:

$$\dot{D} = h_D \dot{\kappa} \exp\left(h_D[\kappa_D - \kappa]\right) = h_D \dot{\kappa}(1-D)$$

where h_D is a ductility parameter.

In our algorithm an incremental approximation of $\dot{D}$ is used, i.e. ΔD is computed from D (and Y), and $\Delta\kappa$ as soon as it is determined from the plastic part of the model resolved in the effective space. For the Lemaitre model the damage rate grows to infinity as D approaches 1 and therefore care should be taken that in the incremental algorithm the computed ΔD does not lead to $D > 1$.

The yield function is now written in terms of effective Kirchhoff stress

$$\phi(\hat{\tau}, \kappa) = \sqrt{2J_2^{\hat{\tau}}} - \sqrt{2/3}q(\kappa) \tag{22}$$

the return mapping is performed, the damage parameter is updated and finally the Kirchhoff stress is computed from eq. (19). The influence of damage on the consistent tangent operator is also included, cf. [2].

Below, we summarize the employed computation algorithm.

Given: deformation gradient $\mathbf{F}_n$, elastic left Cauchy-Green tensor $\mathbf{b}^{\mathrm{e}}_n$, plastic strain measure κ_n, damage D_n at the end of previous step, current update of deformation gradient $\mathbf{F}$ at time $t \equiv t_{n+1}$. Find: Cauchy stress σ, plastic strain measure κ, damage D, tangent operator $\mathbf{D}$ at the end of the current time step $n+1$.

Compute:

1. Incremental deformation gradient $\mathbf{f}$
$$\mathbf{f} = \mathbf{F}\mathbf{F}_n^{-1} \tag{23}$$

2. Trial elastic left Cauchy-Green tensor $\mathbf{b}^{\mathrm{e}}_{tr}$ and its spectral representation using principal stretches $\lambda^{\mathrm{e}}_{A,tr}$ and directions $\mathbf{n}_A$, A=1,2,3
$$\mathbf{b}^{\mathrm{e}}_{tr} = \mathbf{f}\mathbf{b}^{e}_{n}\mathbf{f}^{\mathbf{T}} \tag{24}$$
$$\mathbf{b}^{\mathrm{e}}_{tr} = \sum_{A=1}^{3} \left\{ \left(\lambda^{\mathrm{e}}_{A,tr}\right)^2 \mathbf{n}_A \otimes \mathbf{n}_A \right\} \tag{25}$$

   (starting from here all tensors are written as vectors in principal directions)

3. Trial elastic Hencky strain $\varepsilon^{\mathrm{e}}_{A,tr}$
$$\varepsilon^{\mathrm{e}}_{A,tr} = \log\left(\lambda^{\mathrm{e}}_{A,tr}\right) \tag{26}$$

4. Volumetric and deviatoric part of trial elastic strain Θ_{tr} and $\varepsilon'^{\mathrm{e}}_{A,tr}$
$$\Theta_{tr} = \sum_{A=1}^{3} \varepsilon^{\mathrm{e}}_{A,tr}, \quad \varepsilon'^{\mathrm{e}}_{A,tr} = \varepsilon^{\mathrm{e}}_{A,tr} - \frac{1}{3}\Theta_{tr} \tag{27}$$

5. Trial effective Kirchhoff stress $\hat{\tau}_{A,tr} = \hat{\tau}'_{A,tr} + \hat{p}$
$$\hat{p}_{tr} = K\Theta_{tr}, \quad \hat{\tau}'_{A,tr} = 2G\varepsilon'^{\mathrm{e}}_{A,tr}, \quad \hat{\tau}_{A,tr} = \hat{\tau}'_{A,tr} + \hat{p}_{tr} \tag{28}$$

6. Check yield condition
$$\phi = \sqrt{\hat{\tau}'_{tr}\hat{\tau}'_{tr}} - \sqrt{\frac{2}{3}}q, \quad q = \sigma_{\mathrm{y}} + h\kappa \tag{29}$$

   If $\phi > 0$ then plastic $\rightarrow$ return mapping, compute $\hat{\tau}_A$ and $\Delta\kappa$
   If $\phi < 0$ then elastic $\rightarrow \hat{\tau}_A = \hat{\tau}_{A,tr}$, $\Delta\kappa = 0$

7. Damage update

$$\text{If } \kappa > \kappa_D \text{ then } \Delta D = \Delta D(\Delta\kappa, D, Y), \quad D = D_n + \Delta D \leq 1 \quad \text{else } D = D_n \tag{30}$$

8. Kirchhoff stress τ

$$\tau_A = (1-D)\hat{\tau}_A \tag{31}$$

9. Cauchy stress tensor σ

$$\sigma = \frac{1}{J}\sum_{A=1}^{3}\{(\tau_A)\,\mathbf{n}_A \otimes \mathbf{n}_A\} \tag{32}$$

10. Tangent operator $\mathbf{D}$.

4. Computational tests

In order to assess the performance of damage plasticity coupling theory at large strain some results of numerical experiments are presented. The numerical simulations were performed in FEAP using two-dimensional, displacement-based, isoparametric finite elements. In the first test we analyse uniaxial tension of a one-element specimen, in the second test a perforated plate is considered. Perfect plasticity (no hardening $h = 0$) is assumed. In both tests elastic and plastic material data are the same and they are adopted as follows: elastic modulus $E = 10^4$MPa, Poisson's ratio $\nu = 0{,}3$, yield stress $\sigma_y = 100$MPa. The base values of material parameters related to damage are $\kappa_D = 0.05$, $Y_0 = 0.01$MPa and $h_D = 10$.

4.1. One-element uniaxial tension test

We first consider a square sample with a dimensions 1×1 mm and unit thickness. The applied boundary conditions reproduce uniaxial stresses in tension. One finite element is used for discretization (see Fig. 2).

The diagrams showing the sum of reaction forces on the supported left edge of the sample versus the displacement imposed at the right edge are presented in Figs 3-6. In Figure 3 the differences between pure plasticity and coupled damage-plasticity models is displayed.

It can be observed that the perfect plasticity model at large strain shows softening during the plastic deformation, so unlike for small strains there is no horizontal plateau in the diagram. As is expected, the coupling of plasticity theory with damage results in stronger softening and the modified model is more ductile than the Lemaitre model.

In Figures 4-6 the results obtained for the three different damage-plasticity models are presented. It is shown in Figs 4-6 on the left how the ductility of post-peak response depends on the energy strength of damage Y_0 in the case of the first two coupling options, and on parameter h_D for the exponential model. On the right we can see how the coupling activation depends on the damage threshold κ_D.

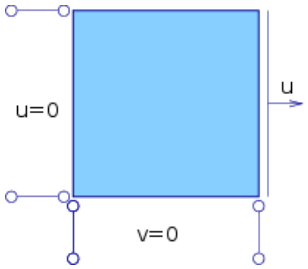

Fig. 2. Uniaxial tension test, one-element discretization, boundary conditions
Rys. 2. Test jednoosiowego rozciągania, 1 element skończony, warunki brzegowe

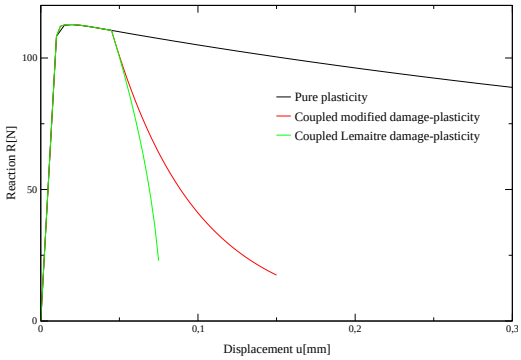

Fig. 3. Reaction sum versus displacement for pure plastic and coupled models
Rys. 3. Wykresy suma reakcji - przemieszczenie otrzymane dla modelu idealnie plastycznego i dwu modeli sprzężonych

4.2. Perforated plate tension test

In the second test a rectangular perforated plate with dimensions 36×20 mm, thickness 1mm and a circular hole with diameter 10mm in the centre is analyzed. The plate is subject to vertical tensile tractions on the upper and lower edges. Because of double symmetry the computations are performed for a quarter of the specimen. The modified damage-plasticity coupling according to eq. (21) is used. The geometry and finite element discretization are presented in Fig. 7. On the left and bottom edges symmetry conditions are applied. The loading is controlled by the displacement of the upper edge.

In Figure 8 we can see a similar behaviour as in the one-element tension test. Both the pure plasticity and the coupled model exhibit softening, after damage initiation the softening becomes stronger. However, in this test strain localization may be observed because of material instability caused by damage. This involves the loss of well-posedness of the mathematical model (loss of

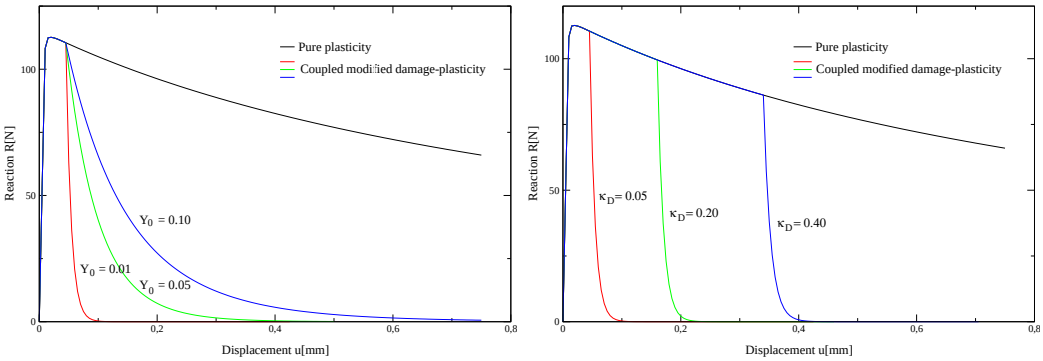

Fig. 4. Reaction sum versus displacement for different parameters of modified damage-plasticity coupling

Rys. 4. Wykresy suma reakcji - przemieszczenie dla różnych parametrów zmodyfikowanego modelu uszkodzenia sprzężonego z plastycznością

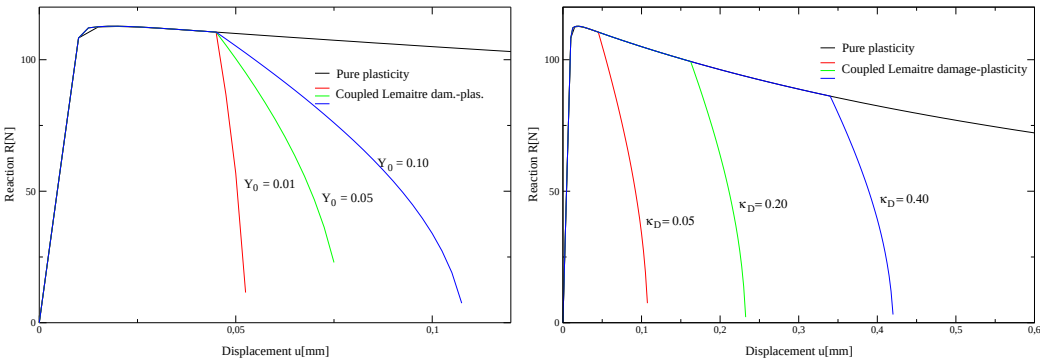

Fig. 5. Reaction sum versus displacement for Lemaitre coupling

Rys. 5. Wykresy reakcje-przemieszczenie dla modelu uszkodzenia Lemaitre'a sprzężonego z plastycznością

ellipticity), which results in uncontrolled damage growth along the horizontal symmetry axis and divergence of computations. It is necessary to regularize the formulation. Figure 8 presents the deformed model and the distribution of the second invariant of stress deviator at the end of the diagram for the coupled model.

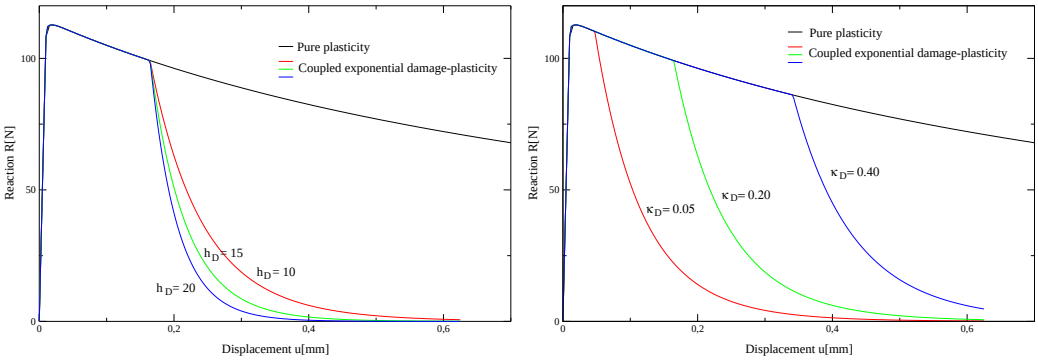

Fig. 6. Reaction sum versus displacement for exponential damage model coupled with plasticity
Rys. 6. Wykresy reakcje-przemieszczenie dla modelu uszkodzenia eksponencjalnego sprzężonego z plastycznością

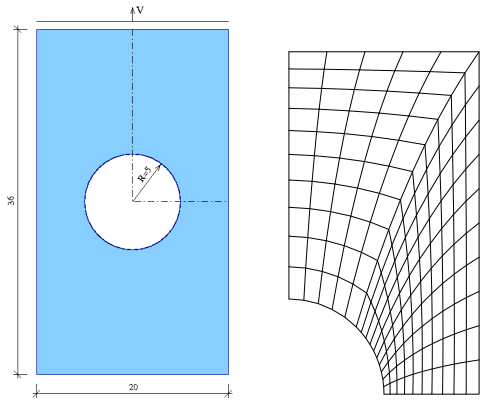

Fig. 7. Perforated plate tension test, FE discretization, boundary conditions
Rys. 7. Test rozciągania płytki z otworem, siatka elementów skończonych, warunki brzegowe

5. Conclusions and regularization proposal

From among various elastic-plastic formulations at large strains the isotropic model based on [1] has been used as the basis for a further extension to damage. It is advantageous from the algorithmic point of view since it preserves the classical return mapping procedure. The coupling to damage is based on the postulate of strain equivalence and effective stresses, and is limited to scalar damage parameter. Three options of damage growth function which determines the coupling have been compared. Two benchmark computations have been performed. In the

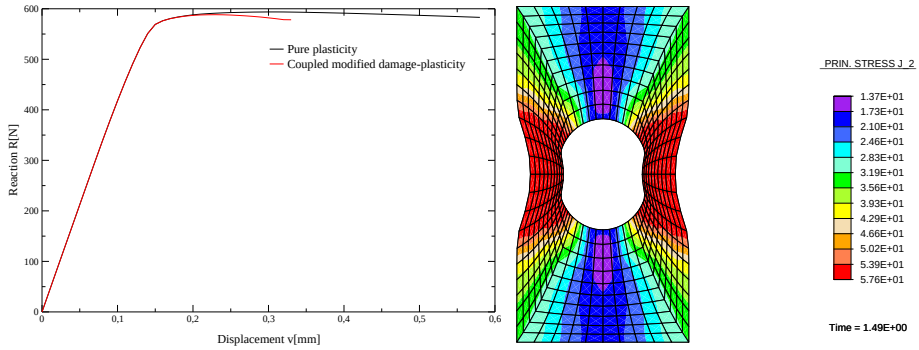

Fig. 8. Reaction sum versus displacement curves for simple damage model coupled with plasticity

Rys. 8. Wykresy suma reakcji - przemieszczenie dla zmodyfikowanego modelu uszkodzenia sprzężonego z plastycznością

perforated plate tension test the loss of material stability may be encountered, so regularization is necessary.

There are many possible enhancements to make the model capable of simulating advanced material damage and strain localization in a proper way, i.e. avoiding a pathological mesh sensitivity of results. It is proposed to use a higher-order continuum model [9]. In the literature one can find for instance:

– implicit averaging of internal parameter κ using the following Helmholtz equation coupled with the equilibrium problem [10]

$$\bar{\kappa} - l_0^2 \nabla_0^2 \bar{\kappa} = \kappa$$

where ∇_0 – gradient computed in the reference configuration and l_0 – internal length scale (the averaged plastic strain measure $\bar{\kappa}$ then determines the damage growth);

– similar implicit averaging of the damage parameter [2]

$$\bar{D} - l_0^2 \nabla_0^2 \bar{D} = D$$

Both these options are computationally advantageous, but each of them requires the discretization of the additional field of plastic multiplier and damage parameter, respectively, which results in a two-field finite element formulation.

The results reported in the paper have been obtained within the framework of the research project No. N501 013 32/1520 supported by Ministry of Science and Higher Education of Poland. The authors also thank the Alexander von Humboldt Foundation for the financial support in the form of equipment and book donation.

References

[1] Auricchio F., Taylor R.L., *A return-map algorithm for general associative isotropic elasto-plastic materials in large deformation regimes*, Int. J. Plasticity, 15:1359–1378, 1999.

[2] Areias P.M.A., de Sa J.M.A.C., Antonio C.A.C., *A gradient model for finite strain elastoplasticity coupled with damage*, Finite Elements in Analysis and Design, 39(13):1191–1235, 2003.

[3] Simo J., *Algorithms for static and dynamic multiplicative plasticity that preserve the classical return mapping schemes of the infinitesimal theory*, Comput. Methods Appl. Mech. Engrg., 99:61–112, 1992.

[4] Bonet J., Wood R.D., *Nonlinear continuum mechanics for finite element analysis*, Cambridge University Press, Cambridge, 1997.

[5] Zienkiewicz O.C., Taylor R.L., *The Finite Element Method for Solid and Structural Mechanics*, Elsevier Butterworth-Heinemann, 6^th edition, 2005.

[6] Żebro T., Pamin J., *An isotropic coupled damage-plasticity model at large strain* (in Polish), in: J. Kubik, W. Kurnik, W.K. Nowacki, eds. *Proc. I Congress of Polish Mechanics*, Abstract p. 153, Warsaw, 2007. Publishing House of Warsaw University of Technology, Paper on CDROM (9 p.).

[7] Lemaitre J., Chaboche J.-L., *Mechanics of Solid Materials*, Cambridge University Press, Cambridge 1990.

[8] Steinmann P., *Formulation and computation of geometrically non-linear gradient damage*, Int. J. Numer. Meth. Engng, 46(5):757–779, 1999.

[9] Pamin J., *Gradient-enhanced continuum models: formulation, discretization and applications*, Series Civil Engineering, Monograph 301, Cracow University of Technology, Cracow 2004.

[10] Geers M.G.D., Ubachs R.L.J.M., Engelen R.A.B., *Strongly non-local gradient-enhanced finite strain elastoplasticity*, Int. J. Numer. Meth. Engng, 56(14):2039–2068, 2003.